DOI: 10.6060/ivkkt.20246701.6721

УДК: 537.525

О ВЛИЯНИИ КИСЛОРОДА НА КИНЕТИКУ ПЛАЗМОХИМИЧЕСКИХ ПРОЦЕССОВ В СМЕСЯХ $CF_4 + O_2$ И $C_4F_8 + O_2$

А.М. Ефремов, Д.Е. Башмакова, K.-H. Kwon

Александр Михайлович Ефремов (ORCID 0000-0002-9125-0763)*, Дарья Евгеньевна Башмакова

Ивановский государственный химико-технологический университет, Шереметевский просп., 7, Иваново, Российская Федерация, 153000
E-mail: amefremov@mail.ru*

Kwang-Ho Kwon (ORCID 0000-0003-2580-8842)

Korea University, 208 Seochang-Dong, Chochiwon, Korea, 339-800
E-mail: kwonkh@korea.ac.kr

Проведено сравнительное исследование электрофизических параметров плазмы, концентраций активных частиц и кинетики атомов фтора в смесях $CF_4 + O_2$ и $C_4F_8 + O_2$ при варьировании их начального состава в условиях постоянства давления газа и вкладываемой мощности. При совместном использовании методов зондовой диагностики и моделирования плазмы подтверждены известные особенности состава плазмы в индивидуальных фторуглеродных газах, а также выявлены ключевые плазмохимические процессы, определяющие параметры и состав газовой фазы в присутствии кислорода. Установлено, что увеличение содержания кислорода при пропорциональном снижении доли фторуглеродного компонента в обеих смесях а) сопровождается относительно слабыми изменениями параметров электронной и ионной компонент плазмы; б) вызывает более быстрое (по сравнению с эффектом разбавления) снижение концентраций фторуглеродных радикалов из-за их окисления в соединения вида CF_xO, FO и CO_x: и в) оказывает существенное влияние на кинетику образования и гибели атомов фтора. Немонотонное (с максимумом при ~ 40-50% O_2) поведение данной величины в смеси $CF_4 + O_2$ обусловлено аналогичным изменением суммарной скорости образования атомов из-за вклада процессов с участием CF_xO и FO. Монотонный рост (с участком постоянства до ~ 40-50% O_2) концентрации атомов фтора в смеси $C_4F_8 + O_2$ не согласуется с изменением скорости их образования, но является следствием снижения частоты гибели атомов в объемных атомно-молекулярных процессах. Проведен предиктивный анализ кинетики гетерогенных процессов с использованием расчетных данных по плотностям потоков активных частиц. Показано, что а) добавка кислорода снижает полимеризационную способность плазмы и б) система $C_4F_8 + O_2$ отличается более высокой полимеризационной способностью при любом фиксированном составе смеси.

Ключевые слова: CF_4, C_4F_8, O_2, плазма, параметры, активные частицы, ионизация, диссоциация, травление, полимеризация

ON THE EFFECT OF OXYGEN ON PLASMA CHEMICAL KINETICS IN $CF_4 + O_2$ AND $C_4F_8 + O_2$ GAS MIXTURES

A.M. Efremov, D.E. Bashmakova, K.-H. Kwon

Alexander M. Efremov (ORCID 0000-0002-9125-0763)*, Daria E. Bashmakova

Ivanovo State University of Chemistry and Technology, Sheremetevskiy ave., 7, Ivanovo, 153000, Russia
E-mail: amefremov@mail.ru*

Kwang-Ho Kwon (ORCID 0000-0003-2580-8842)

Korea University, 208 Seochang-Dong, Chochiwon, Korea, 339-800
E-mail: kwonkh@korea.ac.kr

In this work, we performed the comparative study of electro-physical plasma parameters, densities of active species and fluorine atom kinetics in $CF_4 + O_2$ and $C_4F_8 + O_2$ gas mixtures with variable initial compositions at constant gas pressure and input power. The combination of plasma diagnostics by Langmuir probes and plasma modeling confirmed known features of plasma properties in individual fluorocarbon gases as well as allowed one to figure out key chemical processes determining plasma parameters in the presence of oxygen. It was shown that an increase in O_2 content with a proportional decrease in the fraction of any fluorocarbon component a) causes relatively weak changes in electrons- and ions-related plasma parameters; b) results in more drastic (compared with the dilution effect) decrease in densities of fluorocarbon radicals due to their oxidation into CF_xO, FO and CO_x compounds; and c) sufficiently influences both formation and decay kinetics of fluorine atoms. The non-monotonic (with a maximum at ~ 40-50% O_2) change in the F atom density in the $CF_4 + O_2$ plasma repeats behavior of their formation rate after the contribution of processes involving CF_xO и FO species. The monotonic increase (with a constancy region up to ~ 40-50% O_2) in the F atom density in the $C_4F_8 + O_2$ plasma contradicts with the change in their formation rate, but results from decreasing decay frequency in gas-phase atom-molecular processes. The predictive analysis of heterogeneous process kinetics was carried out using model-yielded data on fluxes of plasma active species. It was found that a) the addition of oxygen always lowers the plasma polymerizing ability; and b) the $C_4F_8 + O_2$ plasma keeps the higher polymerizing ability at any feed gas composition.

Key words: CF_4, C_4F_8, O_2, plasma, parameters, active species, ionization, dissociation, etching, polymerization

Для цитирования:

Ефремов А.М., Башмакова Д.Е., Kwon K.-H. О влиянии кислорода на кинетику плазмохимических процессов в смесях $CF_4 + O_2$ и $C_4F_8 + O_2$. *Изв. вузов. Химия и хим. технология*. 2024. Т. 67. Вып. 1. С. 51–59. DOI: 10.6060/ivkkt.20246701.6721.

For citation:

Efremov A.M., Bashmakova D.E., Kwon K.-H. On the effect of oxygen on plasma chemical kinetics in $CF_4 + O_2$ and $C_4F_8 + O_2$ gas mixtures. *ChemChemTech* [*Izv. Vyssh. Uchebn. Zaved. Khim. Khim. Tekhnol.*]. 2024. V. 67. N 1. P. 51–59. DOI: 10.6060/ivkkt.20246701.6721.

INTRODUCTION

Gaseous fluorocarbons are frequently used plasma-forming environments for the “dry” patterning (partial removal) of silicon and silicon-based materials during the production of the micro- and nano-electronic devices [1-3]. The most popular tool here is the reactive-ion etching (RIE) process that combines the chemical etching (the gasification of surface atoms in a form of volatile fluorides) and the physical sputtering of the treated surface. Accordingly, usual RIE conditions suggest low gas pressures ($p < 20$ mTorr), high input power densities ($w \sim 0.1$ W/cm^3) in order to produce high ionization degrees for gas species as well as high ion bombardment energies ($\varepsilon_i > 100$ eV) in order to exceed typical sputtering thresholds [4, 5].

The specific feature of all fluorocarbon gas plasmas is the surface polymerization effect provided by non-saturated CF_x radicals. This causes the formation of continuous fluorocarbon polymer film on the etched surface while the film thickness influences etching kinetics and output RIE characteristics, such as etching rate, etching selectivity in respect to over- and under-layer materials and etching profile [6-8]. From many published works, it can be understood that a) the polymerizing ability for any fluorocarbon gas plasma strongly depends on the z/x ratio in the original $C_xH_yF_z$ molecule; and b) being used for RIE of Si and SiO_2, CF_4 and C_4F_8 plasmas can be considered as gas systems with a somewhat opposite properties. In particular, the plasma in CF_4 (z/x = 4) provides high etching rates and good surface clearness, but suffers from the nearly isotropic etching profile for Si and low SiO_2/Si etching selectivity [1, 6, 7]. The reason is the low polymerizing ability due to the high density of F atoms and the low density of CF_x (x = 1, 2) radicals. On the contrary, the C_4F_8 plasma (z/x = 2) exhibits the much higher polymerizing ability because of $[CF_x]/[F] > 1$ [9, 10]. That is why the corresponding RIE process combines relatively low etching rates (due to the presence of thick fluorocarbon polymer film on the etched surface), anisotropic etching profiles (due to the protection of side walls by the polymer film) [4, 6, 7] and high SiO_2/Si etching selectivity (due to the thinner polymer film on the oxygen-containing surface that leads to the better access for F atoms) [6, 8].

The effective method to adjust the etching/polymerization balance for the purpose of given RIE process is to combine the fluorocarbon gas with additive component which suppresses the polymerization. From Refs. [10-13], it can be understood that the addition of O_2 always lowers the density of CF_x radicals in a gas phase through the $CF_x + O/O(^1D) \rightarrow CF_{x-1}O + F$ reaction family as well as causes the oxidative destruction of deposited polymer film. At the same time, in spite of numerous works dealt with $CF_4 + O_2$ plasmas, other fluorocarbon gases received much less attention. In particular, the C_4F_8 was mainly studied either in the oxygen-less C_4F_8 + Ar gas mixtures [9, 14-16] or as a component of $C_4F_8 + Ar + O_2$ plasma with variable Ar/O_2 mixing ratio [12, 17, 18]. In last works, the mixture always contained the constant 50% amount of C_4F_8, so that chemical reactions with a participation of oxygen atoms occurred under an excess of the fluorocarbon component. Obviously, such situation does not provide the complete understanding of all possible oxygen-related effects in C_4F_8 - based plasmas. In our previous work [19], we have attempted the model-based study of plasma parameters and composition in $C_4F_8 + O_2$ plasma as a function of component mixing ratio. Unfortunately, the rather applied purpose of that work did not assume the detailed analysis of plasma chemistry as well as required densities of active species only to explain surface modification effects. As a result, the obtained increase in F atom density at 0-80% O_2 was simply attributed to an increase in their formation rate due to $CF_x + O/O(^1D) \rightarrow CF_{x-1}O + F$ processes. In fact, this was just postulated taking in mind existing results for the $CF_4 + O_2$ gas system [4, 11]. At the same time, several recent studies [9, 10, 15, 16] surely demonstrated that steady-state densities of F atoms in CF_4- and C_4F_8 - based plasmas are controlled by different chemical processes. Therefore, any direct analogies between $CF_4 + O_2$ and $C_4F_8 + O_2$ plasmas do not reflect adequately the situation in the last one and thus, are not useful for the corresponding RIE process optimization.

The main idea of this work was to perform the comparative study of $CF_4 + O_2$ and $C_4F_8 + O_2$ plasmas under one and the same operating conditions as well as in a wide range of fluorocarbon/oxygen mixing ratios. In this couple, the $CF_4 + O_2$ plasma also played a role of a reference system with the well-studied chemical reaction mechanisms. Accordingly, main research efforts were focused on such questions as 1) to compare the influence of fluorocarbon/oxygen mixing ratios on electrons- and ions related plasma parameters; 2) to figure out peculiarities of fluorine atom kinetics in both O_2-excess and O_2-deficient reaction regimes; and 3) to analyze how differences in gas-phase plasma parameters and densities of active species may affect the RIE process characteristics.

EXPERIMENTAL AND MODELING DETAILS

Experimental setup and procedures

Plasma diagnostics experiments were carried out in the inductively coupled plasma (ICP) reactor described in our previous works [15, 16]. Plasma was excited using the 13.56 MHz power supply while another 13.56 MHz rf generator powered the bottom electrode in order to produce the negative dc bias voltage ($-U_{dc}$). The latter was to control the ion bombardment energy (ε_i). Constant processing parameters were represented by gas pressure (p = 6 mTorr), input power (W_{inp} = 700 W) and bias power (W_{dc} = 200 W). The condition W_{dc} = const corresponded to the non-constant $-U_{dc}$ because the latter was sensitive to the ion flux. As variable parameters, we used CF_4/O_2 and C_4F_8/O_2 mixing ratios which were set by adjusting partial flow rates for component gases within the constant total flow rate (q) of 40 sccm. Accordingly, an increase of $q(O_2)$ in the range of 0-30 sccm corresponded to the growth of oxygen fraction $y(O_2) = q(O_2)/q$ from 0-75%. Simultaneously, the proportional decrease in the fluorocarbon gas fraction took place.

For plasma diagnostics, we used the double Langmuir probe tool (DLP2000, Plasmart Inc.). The probe head was installed through the viewport on the chamber side wall by ~ 5 cm above the bottom electrode and was centered in the radial direction. In order to reduce the distortion of experimental data due to the deposition of fluorocarbon polymer on probe tips, these were cleaned in 50% Ar + 50% O_2 plasma before and after each measurement. Our previous works [9, 10] have confirmed the efficiency of such procedure to obtain quite reasonable plasma diagnostics data in high polymerizing fluorocarbon gases. The treatment of measured current-voltage (I-V) curves was based on well-known statements of Langmuir probe theory for low pressure plasmas [4, 20]. As a result, we obtained data on electron temperature (T_e), ion current density (J_+) and total density of positive ions (n_+).

Plasma modeling

In order to obtain data on steady-state densities and fluxes of plasma active species, we applied a simplified 0-dimensional (global) plasma model. The model content and approaches were identical to those used in our previous works dealt with various low-pressure ($p < 20$ mTorr) and high-density ($n_+ > 10^{10}$ cm^{-3}) fluorocarbon gas plasmas [15-18]. In particular, it was assumed that:

1) The electron energy distribution function (EEDF) is featured by the nearly Maxwellian shape. This fact has several experimental confirmations [11, 14, 21-23] and is caused by the essential contribution of electron-electron collisions to the overall electron energy loss. Accordingly, rate coefficients for electron-impact processes were found using fitting expressions $k = f(T_e)$ [21, 22] obtained after the integration of Maxwellian EEDF with corresponding process cross-sections.

2) The electronegativity of CF_4, C_4F_8 and O_2 plasmas is low enough to equalize the total density of positive ions n_+ with the electron density n_e. Such situation is provided by high ionization degree of gas species ($n_+/N > 10^{-4}$, where $N = p/k_BT_g$ is the total gas density at the gas temperature of T_g) and low efficiency of electron attachment processes at low pressures.

3) The parameter T_g keeps the nearly constant value under the condition of p, W = const. Since experimental data on T_g were not available in this study, we used the value of 600 K which is quite typical for given processing conditions, reactor type and geometry [15, 16].

4) The recombination of atoms and radicals on chamber walls follows the first-order kinetics with the rate coefficient of $k \approx (r+l)\gamma\upsilon_T/2rl$, where r and l are inner sizes of the cylindrical reactor chamber, υ_T is the thermal velocity of target species and γ is their recombination probability [22, 23].

Sets of chemical reaction with corresponding rate coefficients were taken from our previous works dealt with the modeling of $CF_4 + Ar + O_2$ [11, 13] and $C_4F_8 + Ar + O_2$ [12, 13, 18] plasmas. In fact, we used the well-adjusted kinetic schemes which previously have been tested by several authors and demonstrated the good agreement between measured and model-predicted plasma parameters [11, 12, 14]. In order to avoid both repetitions and excess data, we decided not to publish the full reaction table which includes more than 100 processes. Instead, the discussion below will mostly operate by generalized groups of process which are featured by the real influence to the kinetics of selected species.

RESULTS AND DISCUSSION

From Table 1, it can be seen that an increase in $y(O_2)$ in both gas mixtures causes different changes in electron temperature as well as produces quite similar effects on both total density of positive ions and ion current density characterizing the ion flux $\Gamma_+ \approx J_+/e$. These results may briefly be explained as follows:

- In the $CF_4 + O_2$ plasma, a weak increase in T_e with increasing O_2 fraction in a feed gas is surely connected with the change of dominant neutral gas-phase component from original CF_4 molecules to F atoms, as shown in Fig. 1(a). Since collisions of electrons with molecular species are characterized by higher energy losses for both excitation (due to the low-threshold vibrational and electronic states) and ionization (due to generally higher ionization cross-sections for bigger-sized particles), such situation corresponds to decreasing overall electron energy losses and increasing mean electron energy $<\varepsilon> = 3/2T_e$. Another important feature is that the rate coefficient for R1: $F + e \rightarrow F^+ + 2e$ ($\sim 7.8 \cdot 10^{-11}$ cm^3/s at $T_e = 3.7$ eV) is much lower compared with R2: $CF_x + e \rightarrow CF_{x-1}^+ + F + 2e$ for x = 4 ($\sim 3.8 \cdot 10^{-10}$ cm^3/s at $T_e = 3.7$ eV). Therefore, a decrease in J_+ toward O_2-rich plasmas directly reflects the same behavior of n_+ due to a decrease in the total ionization rate. Taking into account the low electronegativity of both CF_4 and O_2 plasmas at $p < 20$ mTorr [11, 21, 24], the identical change for $n_e = f(y(O_2))$ also takes place.

- In the $C_4F_8 + O_2$ plasma, a monotonic decrease in T_e toward higher $y(O_2)$ values may surely be related to increasing electron energy losses in low-threshold excitations processes for molecular products of plasma chemical reactions, such as CF_4, CF_2O, CO and CO_2 (Fig. 1(b)). Accordingly, the decreasing mean electron energy lowers ionization rate coefficients for neutral species and thus, reduces formation rates for electrons and positive ions in O_2-rich plasmas. In addition, the appearance of more electronegative oxygen-containing species may accelerate loss rates for electrons and positive ions through the dissociative attachment and ion-ion recombination, respectively. As such, a decreasing tendency for $J_+ = f(y(O_2))$ obtained in experiments is also caused by the corresponding change in n_+.

The common feature of both gas systems is that the addition of O_2 leads to an increase in the negative dc bias voltage $-U_{dc}$ at the constant bias power (Table 1). The reason is that the decreasing ion flux weakens the compensation for the excess negative charge produced by the bias power source. However, the corresponding change on the ion bombardment energy (ε_i = 285-303 eV for $CF_4 + O_2$ and 306-309 eV for $C_4F_8 + O_2$ at 0-75% O_2) is essentially weaker compare with the opposite tendency of Γ_+. As a result, the parameter $G1 = (M_i\varepsilon_i)^{1/2}\Gamma_+$ characterizing the ion bombardment intensity [9, 10] always demonstrates the monotonic decrease toward O_2-rich plasmas (Table 1).

Table 1

Electrons- and ions-related plasma parameters

***Таблица 1.* Параметры электронной и ионной компонент плазмы**

$y(O_2)$, %	T_e, eV	J_+, mA/cm^2	$n_+ \approx n_e$, 10^{10} cm^{-3}	$-U_{dc}$, V	G1, 10^{17}
$CF_4 + O_2$					
0	3.56	0.95	4.37	262	8.32
25	3.65	0.94	3.56	268	6.93
50	3.79	0.93	3.02	275	6.08
75	3.96	0.92	2.62	280	5.43
$C_4F_8 + O_2$					
0	4.70	1.05	3.91	278	8.89
25	4.56	1.02	3.32	280	7.45
50	4.40	0.98	2.90	282	6.39
75	4.22	0.95	2.58	284	5.64

Note: $G1 = (M_i\varepsilon_i)^{1/2}\Gamma_+$, eV$^{1/2}$cm^{-2}s^{-1}

Примечание: $G1 = (M_i\varepsilon_i)^{1/2}\Gamma_+$, эВ$^{1/2}$см$^{-2}$с$^{-1}$

When analyzing kinetics of neutral species in oxygen-less gas systems, we reasonably obtained the most of features known from previous works [15-17, 21, 25]. In particular, it was found that dominant gas-phase components in pure CF_4 plasma are original CF_4 molecules, CF_3 radical and fluorine atoms with the condition of $[CF_4] > [CF_3] \approx [F]$ (Fig. 1(a)). Reactions R2 for x = 4 and R3: $CF_x + e \rightarrow CF_{x-1} + F + e$ for x = 3, 4 compose ~ 80% of the total F atom formation rate (Fig. 2(a)) while contributions of both R2 for $x < 4$ and R4: $CF_x + e \rightarrow CF_{x-2} + 2F + e$ are almost negligible due to either low rate coefficients or low densities of source species. From Fig. 2(a), it can be seen also that ~10% of total F atom formation rate comes from R5: $F_2 + e \rightarrow$ $\rightarrow 2F + e$. The latter is due to the high rate coefficient ($k_5 \sim 2.2 \cdot 10^{-9}$ cm^3/s vs. $k_2 \sim 5.4 \cdot 10^{-10}$ cm^3/s) and the essential density of F_2 molecules provided by the effective R6: $F + F \rightarrow F_2$ on chamber walls. Accordingly, the last process in a combination with R7: $F + CF_x \rightarrow$ $\rightarrow CF_{x+1}$ represent the main loss pathway for fluorine atoms.

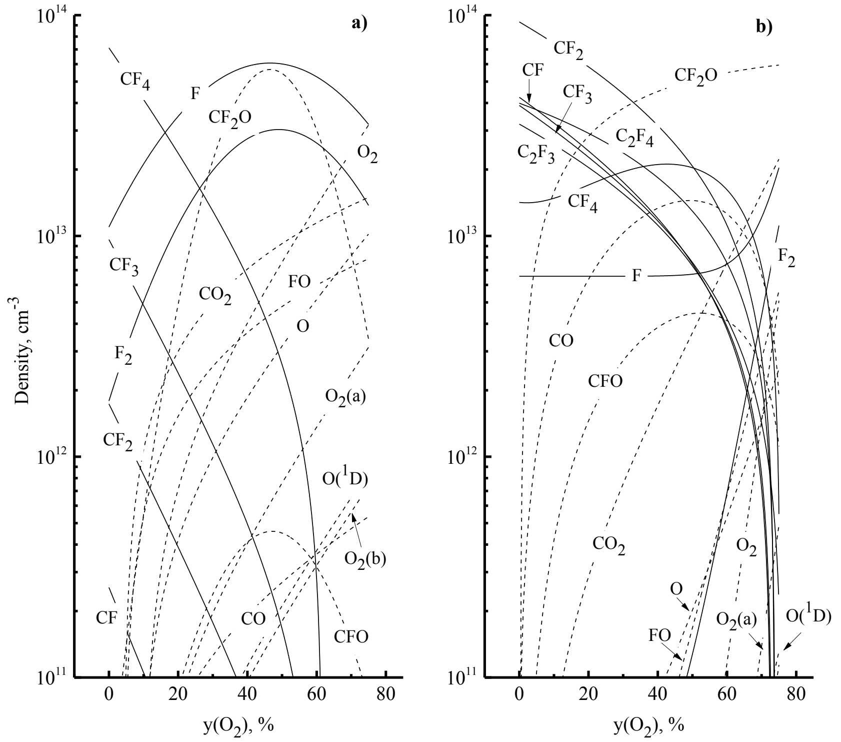

Fig. 1. Steady-state densities of neutral species in $CF_4 + O_2$ (a) and $C_4F_8 + O_2$ (b) plasmas. Curves marked as $O_2(a)$ and $O_2(b)$ correspond to metastable states of $O_2(a^1\Delta)$ and $O2(b^1\Sigma)$, respectively

Рис. 1. Стационарные концентрации нейтральных частиц в плазме $CF_4 + O_2$ (a) and $C_4F_8 + O_2$ (b). Метки на кривых $O_2(a)$ и $O_2(b)$ обозначают метастабильные состояния $O_2(a^1\Delta)$ и $O_2(b^1\Sigma)$, соответственно

In the C_4F_8 plasma, the gas phase is mostly composed by non-saturated fluorocarbon radicals CF_x (x = 1, 2, 3) and C_2F_x (x = 3, 4) (Fig. 1(b)). These particles appear due to the fragmentation of original C_4F_8 molecules in R8: $C_4F_8 + e \rightarrow 2C_2F_4 + e$ and R9: $C_4F_8 + e \rightarrow C_3F_6 + CF_2 + e$ as well as result from the further decomposition of corresponding reaction products through R3 for x = 2, R10: $C_3F_6 + e \rightarrow C_2F_4 + CF_2 +$ $+ e$, R11: $C_2F_4 + e \rightarrow 2CF_2 + e$ and R12: $C_2F_4 + e \rightarrow$ $\rightarrow C_2F_3 + F + e$. Accordingly, the main source of F atoms is R3 for x = 1-3 (Fig. 2(b)) while their decay in addition to R6 and R7 is noticeably contributed by

R13: $C_2F_4 + F \rightarrow CF_2 + CF_3$ ($k_{13} \sim 4.0 \cdot 10^{-11}$ cm^3/s). Due to the last process, the C_4F_8 plasma exhibits lower [F] value (Fig.1) thought is characterized by higher F atom formation rate (Fig. 2).

The substitution of CF_4 for O_2 in the $CF_4 + O_2$ gas mixture rapidly lowers densities of CF_x radicals due to their conversion into CF_2O, CFO, CO and CO_2 species (Fig. 1(a)) in R14: $CF_x + O/O(^1D) \rightarrow CF_{x-1}O + F$ ($k_{14} \sim 6.1 \cdot 10^{-11}$ cm^3/s for x = 1 and $\sim 3.2 \cdot 10^{-11}$ cm^3/s for x = 2, 3). The domination of CF_2O over other oxygen-containing reaction products as well as the drastic growth of their density at $y(O_2) < 40\%$ is supported by gas-phase processes R15: $CF_x + CFO \rightarrow CF_2O + CF_{x-1}$ ($k_{15} \sim 1.1 \cdot 10^{-11}$ cm^3/s for x = 2 and $\sim 7.0 \cdot 10^{-13}$ cm^3/s for x = 1), R16: $2CFO \rightarrow CF_2O + CO$ ($k_{16} \sim 1.0 \cdot 10^{-11}$ cm^3/s) and R17: $CFO + F \rightarrow CF_2O$ ($k_{17} \sim 8.0 \cdot 10^{-11}$ cm^3/s). At the same time, the condition $y(O_2) > 40\%$ causes the more than ten-time decrease in [CF_x] (in fact, corresponds to the transition into the fluorocarbon-deficient reaction regime) and thus, reduces rates of R14 and R15. Accordingly, this results in the sharp maximum of the [CF_2O] = f($y(O_2)$) curve, as shown in Fig. 1(a). As for the kinetics of F atoms, an increase in $y(O_2)$ causes two principal effects influencing their total formation rate. First, the transition toward O_2-ruch plasmas increases the density of F_2 molecules (Fig. 1(a)) through both R6 and R18: $CF_2O + O/O(^1D) \rightarrow F_2 + CO_2$ that sufficiently accelerates R5 (Fig. 2(a)). As a result, the rate of R5 exceeds the total effect from R2 and R3 starting from 10-15% O_2 as well as exhibits the maximum at ~ 40% O_2 due to the same change in [F_2]. And secondly, the presence of oxygen adds new F atom formation pathways, such as electron-impact processes R19: $CF_xO + e \rightarrow CF_{x-1}O + F + e$ and R20: $FO + e \rightarrow F + O + e$ as well as atom-molecular reactions R14, R21: $FO + O/O(^1D) \rightarrow O_2 + F$ ($k_{21} \sim 2.5 \cdot 10^{-11}$/$5.0 \cdot 10^{-11}$ cm^3/s), R22: $CFO + O/O(^1D) \rightarrow CO_2 + F$ ($k_{22} \sim 1.0 \cdot 10^{-10}$ cm^3/s) and R23: $F_2 + O/O(^1D) \rightarrow FO + F$ ($k_{23} \sim 2.5 \cdot 10^{-11}$ cm^3/s). From Fig. 2(a), it can be seen that the superposition of R5, R19 and R20 produces the maximum on the total F atom formation rate (and thus, on the F atom density, as shown in Fig. 1(a)) while the contribution of R21 and R22 begins to be noticeable only at $y(O_2) > 60\%$. The stronger effect of $y(O_2)$ on [F] value in the range of 0-40% O_2 is connected with decreasing F atom loss rate in R7.

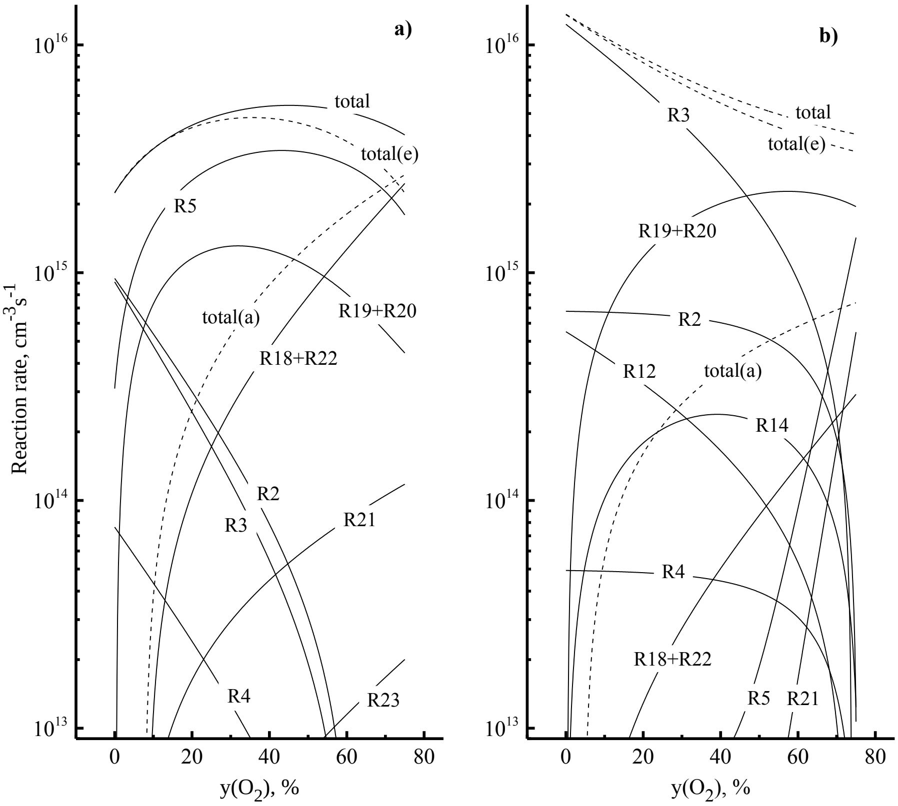

Fig. 2. Fluorine atom formation rates in $CF_4 + O_2$ (a) and $C_4F_8 + O_2$ (b) plasmas. Numerical labels on curves correspond to reaction numbers in the text. Curves marked as "total (e)" and "total (a)" illustrate overall effects from electron-impact and atom-molecular reactions, respectively

Рис. 2. Скорости процессов образования атомов фтора в плазме $CF_4 + O_2$ (a) and $C_4F_8 + O_2$ (b). Числовые метки на кривых соответствуют номеру реакции в тексте статьи. Кривые с метками "total (e)" и "total (a)" иллюстрируют суммарные эффекты от реакций под действием электронного удара и атомно-молекулярных процессов, соответственно

The substitution of C_4F_8 for O_2 in the $C_4F_8 + O_2$ gas mixture also initiates the decomposition of CF_x radicals through R14, but results in much weaker decrease in their densities compared with $CF_4 + O_2$ plasma (Fig. 1). The reason is low densities of O and $O(^1D)$ atoms due to the effective loss of O_2 molecules in R24: $CF + O_2 \rightarrow CFO + O$ ($k_{24} \sim 3.2 \cdot 10^{-11}$ cm^3/s) and R25: $C + O_2 \rightarrow CO + O$ ($k_{25} \sim 1.5 \cdot 10^{-11}$ cm^3/s). Really, since both CO and CO_2 are characterized by much lower dissociation rate coefficients compared with O_2 itself (for example, $\sim 5.2 \cdot 10^{-10}$ cm^3/s for R26: $CO + e \rightarrow C + O + e$ vs. $\sim 3.1 \cdot 10^{-9}$ for R27: $O_2 + e \rightarrow$ $\rightarrow O + O(^1D) + e$), such situation results in sufficiently lower O and $O(^1D)$ formation rates than those in the $CF_4 + O_2$ plasma under identical operating conditions. The lack of oxygen expectedly reduces the significance of R14, R19 and R20 in respect to the production of F atoms in the O_2-rich plasmas while the contribution of R5 is limited by the very low density of F_2 molecules in the C_4F_8-rich plasma. The last phenomenon is due to the effective loss of F_2 in R28: $CF_x + F_2 \rightarrow CF_{x+1} + F$, mainly for x = 1. All these lead to the monotonic decrease in the total F atom formation rate toward higher $y(O_2)$ values, as shown in Fig. 2(b). At the same time, one can also obtain the rapid decrease in the F atom loss frequency in R13 due to the same change in the density of corresponding source species, C_2F_4. The slower fall in $[C_2F_4]$ at $y(O_2) < 50\%$ (by ~ 4 times for 0-50% O_2) just compensates for the opposite tendency in the total F atom formation rate and thus, results in $[F] \approx const$ (Fig. 1(b)). Accordingly, the faster decrease in $[C_2F_4]$ at $y(O_2) > 50\%$ (by more than 1000 times for 50-75% O_2) stronger influences the rate of R13, overlaps a decrease in the total F atom formation rate and causes the growth of F atom density. Therefore, specific features of $C_4F_8 + O_2$ plasma are a) the almost negligible effect of oxygen-related processes on the F atom formation kinetics; and b) the sufficient change in the F atom loss frequency that causes the contradiction between their steady-state density and total formation rate. Therefore, though the model-predicted data on species densities obtained in Ref. [19] are principally correct, the reason providing an increase in [F] in the range of 0-80% O_2 was postulated improperly.

Above data on densities of plasma active species allow one the predictive analysis of the of heterogeneous process kinetics, such as etching and polymerization. The basic principles for such analysis in fluorocarbon-based plasmas have been discussed in our previous works [9, 10, 16-18]. In particular, the influence of processing conditions on the polymer deposition rate be characterized by the parameter $G2 = \Gamma_{pol}/\Gamma_F$, where Γ_{pol} is the flux of polymerizing species (the total flux of fluorocarbon radicals with two and more free bonds), and Γ_F is the flux of F atoms. From Table 2, it can be seen that polymerizing fluxes in both gas systems demonstrate similar decreasing tendencies toward O_2-rich plasma, but exhibit sufficient differences in absolute values at any fixed $y(O_2)$. The latter is directly connected with corresponding differences in densities of CF_2 and CF radicals mentioned in Fig. 1. Accordingly, the combination of higher Γ_{pol} with lower Γ_F reasonably produces much higher (by more than 100 times) G2 values in $C_4F_8 + O_2$ plasma. It is known also that the destruction of the fluorocarbon polymer film in oxygen-containing plasmas is provided by both physical (sputtering by ion bombardment) and chemical (etching by oxygen atoms) pathways. As such, corresponding changes in the steady-state polymer film thickness may be traced by G3 = G2/G1 and $G4 = G2/\Gamma_O$, where Γ_O is the flux of oxygen atoms [17, 18]. The data of Tab. 2 allow one to conclude that these two parameters are always higher in the $C_4F_8 + O_2$, so that this gas system always provides the thicker polymer film and thus, exhibits the higher polymerizing ability compared with $CF_4 + O_2$. Therefore, even an excess of oxygen does not disturb the basic rule found for oxygen-less CF_4 - and C_4F_8 - based plasmas [9, 10, 16].

In addition, the parameter $G5 = \Gamma_F/G1$ may be used to characterize the balance between chaotic and directional etching pathways and thus, to trace the change in the etching anisotropy. As can be seen from Table 2, the growth of G5 with increasing $y(O_2)$ in $CF_4 + O_2$ plasma formally means the worse condition for obtaining the anisotropic etching profile. At the same time, one must remember that the oxygen may passivate the surface of sidewalls through both the oxidation of surface atoms and/or the formation of lower volatile oxygen-containing compounds [10, 18]. Therefore, one can expect that the real change of the etching profile for some materials may be either weaker or even the opposite compared with that predicted by G5. On this background, the nearly constant G5 in the $C_4F_8 +$ $+ O_2$ plasma as well as lower absolute values of this parameters starting from $y(O_2) > 15\text{-}20\%$ surely mean its advantage in respect the anisotropic etching. Though this fact has found numerous experimental evidences for oxygen-less CF_4- and C_4F_8-based plasmas, the reason was the protective effect from the thick fluorocarbon polymer film obtained in the last gas system [4, 6-8]. At the same time, our data suggest the same situation in O_2-rich gas mixtures, when the polymer film has the low thickness and/or even exhibits the non-continuous structure. Obviously, this suggestion needs the experimental approval.

Table 2

Parameters characterizing heterogeneous process kinetics

Таблица 2. **Параметры, характеризующие кинетику гетерогенных процессов**

$y(O_2)$, %	Γ_{pol}, 10^{16} $cm^{-2}s^{-1}$	G2, 10^{-3}	G3, 10^{-20}	G4, 10^{-18}	G5
$CF_4 + O_2$					
0	2.80	121	14.5	-	0.28
25	0.42	3.94	0.57	20.6	1.53
50	0.02	0.01	0.02	0.02	1.92
75	0.007	0.009	0.01	0.001	1.36
$C_4F_8 + O_2$					
0	199	13700	1550	-	0.16
25	110	9130	1220	6370	0.17
50	35.3	2860	447	600	0.19
75	0.15	3.35	0.59	0.05	0.80

Note: $G2 = \Gamma_{pol}/\Gamma_F$; $G3 = G2/G1$, $eV^{-1/2}cm^2s$; $G4 = G2/\Gamma_O$, cm^2s; and $G5 = \Gamma_F/G1$, $eV^{-1/2}$

Примечание: $G2 = \Gamma_{pol}/\Gamma_F$; $G3 = G2/G1$, эВ$^{-1/2}$см^{2}с; $G4 = G2/\Gamma_O$, см^{2}с; and $G5 = \Gamma_F/G1$, эВ$^{-1/2}$

CONCLUSIONS

The aim of this work was to compare electrophysical plasma parameters, densities of active species and fluorine atom kinetics in $CF_4 + O_2$ and $C_4F_8 + O_2$ gas mixtures with variable initial compositions. From plasma diagnostics and modeling data, in was found that an increase in O_2 content in a feed gas in both gas mixtures a) causes relatively weak changes in both electron temperature and electron density; b) results in faster (compared with the dilution effect) decrease in densities of fluorocarbon radicals due to their effective oxidation into CF_xO, FO and CO_x compounds; and c) sufficiently influences the F atom kinetics. In particular, the non-monotonic (with a maximum at ~ 40-50% O_2) change in the F atom density in the $CF_4 + O_2$ plasma follows the behavior of their formation rate which is contributed by processes involving CF_xO и FO species. At the same time, the monotonic increase (with a constancy region up to ~ 40-50% O_2) in the F atom density in the $C_4F_8 + O_2$ plasma contradicts with the change of formation rate, but results from decreasing F atom loss frequency in gas-phase atom-molecular processes. The model-based analysis of heterogeneous process kinetics indicated that the addition of oxygen always lowers the plasma polymerizing ability (through decreasing flux of polymerizing species and accelerating the oxidative destruction of deposited polymer film) while both effects are weaker in the $C_4F_8 + O_2$ plasma. The latter is due to the lack of oxygen atoms caused by effective losses of both O_2 and O species in gas-phase reactions.

The work was supported by the Russian Science Foundation grant № 22-29-00216, https://rscf.ru/project/22-29-00216/.

The authors declare the absence a conflict of interest warranting disclosure in this article.

Исследование выполнено за счет гранта Российского научного фонда № 22-29-00216, https://rscf.ru/project/22-29-00216/.

Авторы заявляют об отсутствии конфликта интересов, требующего раскрытия в данной статье.

REFERENCES
ЛИТЕРАТУРА

1. **Wolf S., Tauber R.N.** Silicon Processing for the VLSI Era. Volume 1. Process Technology. New York: Lattice Press. 2000. 416 p.
2. **Nojiri K.** Dry etching technology for semiconductors. Tokyo: Springer Internat. Publ. 2015. 116 p. DOI: 10.1007/978-3-319-10295-5.
3. Advanced plasma processing technology. New York: John Wiley & Sons Inc. 2008. 479 p.
4. **Lieberman M.A., Lichtenberg A.J.** Principles of plasma discharges and materials processing. New York: John Wiley & Sons Inc. 2005. 757 p. DOI: 10.1002/0471724254.
5. **Donnelly V.M., Kornblit A.** Plasma etching: Yesterday, today, and tomorrow. *J. Vac. Sci. Technol.* 2013. V. 31. P. 050825-48. DOI: 10.1116/1.4819316.
6. **Standaert T.E.F.M., Hedlund C., Joseph E.A., Oehrlein G.S., Dalton T.J.** Role of fluorocarbon film formation in the etching of silicon, silicon dioxide, silicon nitride, and amorphous hydrogenated silicon carbide. *J. Vac. Sci. Technol. A.* 2004. V. 22. P. 53-60. DOI: 10.1116/1.1626642.
7. **Kastenmeier B.E.E., Matsuo P.J., Oehrlein G.S.** Highly selective etching of silicon nitride over silicon and silicon dioxide. *J. Vac. Sci. Technol. A.* 1999. V. 17. P. 3179-3184. DOI: 10.1116/1.58209.
8. **Schaepkens M., Standaert T.E.F.M., Rueger N.R., Sebel P.G.M., Oehrlein G.S., Cook J.M.** Study of the SiO_2-to-Si_3N_4 etch selectivity mechanism in inductively coupled fluorocarbon plasmas and a comparison with the SiO_2-to-Si mechanism. *J. Vac. Sci. Technol. A.* 1999. V. 17. P. 26-37. DOI: 10.1116/1.582108.
9. **Efremov A., Murin D., Kwon K.-H.** Concerning the Effect of Type of Fluorocarbon Gas on the Output Characteristics of the Reactive-Ion Etching Process. *Russ. Microelectronics.* 2020. V. 49. N 3. P. 157-165. DOI: 10.1134/S1063739720020031.
10. **Efremov A., Lee B. J., Kwon K.-H.** On Relationships Between Gas-Phase Chemistry and Reactive-Ion Etching Kinetics for Silicon-Based Thin Films (SiC, SiO_2 and Si_xN_y) in Multi-Component Fluorocarbon Gas Mixtures. *Materials.* 2021. V. 14. P. 1432(1-27). DOI: 10.3390/ma14061432.
11. **Kimura T., Noto M.** Experimental study and global model of inductively coupled CF_4/O_2 discharges. *J. Appl. Phys.* 2006. V. 100. P. 063303 (1-9). DOI: 10.1063/1.2345461.
12. **Chun I., Efremov A., Yeom G. Y., Kwon K.-H.** A comparative study of $CF_4/O_2/Ar$ and $C_4F_8/O_2/Ar$ plasmas for dry etching applications. *Thin Solid Films.* 2015. V. 579. P. 136-143. DOI: 10.1016/j.tsf.2015.02.060.
13. **Efremov A., Lee J., Kim J.** On the Control of Plasma Parameters and Active Species Kinetics in $CF_4 + O_2 + Ar$ Gas Mixture by CF_4/O_2 and O_2/Ar Mixing Ratios. *Plasma*

Chem. Plasma Proc. 2017. V. 37. P. 1445-1462. DOI: 10.1007/s11090-017-9820-z.

14. **Kokkoris G, Goodyear A., Cooke M., Gogolides E.** A global model for C_4F_8 plasmas coupling gas phase and wall surface reaction kinetics. *J. Phys. D. Appl. Phys.* 2008. V. 41. P. 195211 (1-12). DOI: 10.1088/0022-3727/41/19/195211.
15. **Efremov A.M., Murin D.B., Kwon K.H.** Plasma parameters and active species kinetics in CF_4+C_4F_8+Ar gas mixture. *ChemChemTech [Izv. Vyssh. Uchebn. Zaved. Khim. Khim. Tekhnol.].* 2018. V. 61. N 4-5. P. 31-36. DOI: 10.6060/tcct.20186104-05.5695.

    Ефремов А.М., Мурин Д.Б., Квон К.Х. Параметры плазмы и кинетика активных частиц в смеси CF4+C4F8+Ar. *Изв. вузов. Химия и хим. технология.* 2018. Т. 61. Вып. 4-5. С. 31−36.
16. **Efremov A.M., Betelin V.B, Mednikov K.A., Kwon K.H.** Gas-phase parameters and reactive-ion etching regimes for Si and SiO_2 in binary Ar + CF_4/C_4F_8 mixtures. *ChemChemTech [Izv. Vyssh. Uchebn. Zaved. Khim. Khim. Tekhnol.].* 2021. V. 64. N 6. P. 25-34. DOI: 10.6060/ivkkt.20216406.6377.

    Ефремов А.М., Бетелин В.Б., Медников К.А., Kwon K.-H. Параметры газовой фазы и режимы реактивно-ионного травления Si и SiO_2 в бинарных смесях Ar + CF_4/C_4F_8. *Изв. вузов. Химия и хим. технология.* 2021. Т. 64. Вып. 6. С. 25-34.
17. **Lim N., Efremov A., Kwon K.-H.** A comparison of CF_4, CHF_3 and C_4F_8 + Ar/O_2 Inductively Coupled Plasmas for Dry Etching Applications. *Plasma Chem. Plasma Process.* 2021. V. 41. P. 1671-1689. DOI: 10.1007/s11090-021-10198-z.
18. **Lee B. J., Efremov A., Nam Y., Kwon K.-H.** Plasma Parameters and Silicon Etching Kinetics in C4F8 + O_2 + Ar Gas Mixture: Effect of Component Mixing Ratios. *Plasma Chem. Plasma Process.* 2020. V. 40. P. 1365-1380. DOI: 10.1007/s11090-020-10097-9.
19. **Lee J., Kwon K.H., Efremov A., Yeom G.Y.** Silicon Surface Modification Using C_4F_8+O_2 Plasma for Nano-Imprint Lithography. *J. Nanosci. Nanotechnol.* 2015. V. 15. N 11. P. 8749-8755. DOI: 10.1166/jnn.2015.11511.
20. **Shun'ko E.V.** Langmuir probe in theory and practice. Boca Raton: Universal Publ. 2008. 245 p.
21. **Kimura T., Ohe K.** Probe measurements and global model of inductively coupled Ar/CF_4 discharges. *Plasma Sources Sci. Technol.* 1999. V. 8. P. 553-560. DOI: 10.1088/0963-0252/8/4/305.
22. **Rauf S., Ventzek P.L.** Model for an inductively coupled Ar/c-C_4F_8 plasma discharge. *J. Vac. Sci. Technol. A.* 2002. V. 20. P. 14-23. DOI: 10.1116/1.1417538.
23. **Vasenkov A.V., Li X., Oehlein G.S., Kushner M.J.** Properties of c-C_4F_8 inductively coupled plasmas. II. Plasma chemistry and reaction mechanism for modeling of Ar/c-C_4F_8/O_2 discharges. *J. Vac. Sci. Technol. A.* 2004. V. 22. P. 511-530. DOI: 10.1116/1.1697483.
24. **Hsu C.C., Nierode M.A., Coburn J.W., Graves D.B.** Comparison of model and experiment for Ar, Ar/O_2 and Ar/O_2/Cl_2 inductively coupled plasmas. *J. Phys. D. Appl. Phys.* 2006. V. 39. P. 3272-3284. DOI: 10.1088/0022-3727/39/15/009.
25. **Efremov A.M., Bashmakova D.E., Kwon K.-H.** Features of plasma composition and fluorine atom kinetics in CHF_3 + O_2 gas mixture. *ChemChemTech [Izv. Vyssh. Uchebn. Zaved. Khim. Khim. Tekhnol.].* 2023. V. 66. N 1. P. 48-55. DOI: 10.6060/ivkkt.20236601.6667.

    Ефремов А.М., Башмакова Д.Е., Kwon K.-H. Особенности состава плазмы и кинетики атомов фтора в смеси CHF_3 + O_2. *Изв. вузов. Химия и хим. технология.* 2023. Т. 66. Вып. 1. С. 48-55.

Поступила в редакцию 09.09.2022
Принята к опубликованию 17.05.2023

Received 09.09.2022
Accepted 17.05.2023